

Single Top and Light Higgs at TeV Energy γe Colliders

E. Boos^{1,2}, A. Pukhov², M. Sachwitz³ and H. J. Schreiber³

¹Institut für Kernphysik, TU, Darmstadt, FRG

²Institute of Nuclear Physics, Moscow State University, 119899, Moscow,
Russia

³DESY-Institut für Hochenergiephysik, Zeuthen, FRG

Contribution to the Proceedings of the 'ECFA/DESY Study on Physics and Detectors for the Linear Collider', DESY 97-123E, ed. by R. Settles.

Abstract

Results of complete tree level calculation of the single top and light Higgs production in the reaction $\gamma e \rightarrow \nu b \bar{b} W$ at the Next Linear Collider are presented. In addition, the contributions of anomalous operators to the Wtb and WWH couplings are included into the complete 4-body consideration. The sensitivity for probing the structure of the couplings in a model independent way is analyzed.

1 Introduction

The top quark, by far the heaviest established elementary particle, is not only a further confirmation of the Standard Model (SM), but it also poses new questions. One example is the spectacular numerical coincidence between the vacuum expectation value $v/\sqrt{2} = 175$ GeV and the top quark mass, measured by the CDF and D0 collaborations [1] to be 175^{+6}_{-6} GeV, and extracted indirectly from fits of precision electroweak LEP data as 177^{+7+16}_{-7-19} GeV [2]. It is an open question whether or not this is due to fundamental physics relations or is only accidental. The heavy top quark decays electro-weakly before hadronization [3] and therefore it could provide a first window to help understand the nature of the electroweak symmetry breaking [4]. In this context, reactions involving a light Higgs boson and top quark production as intermediate states are extremely interesting. One example is the reaction $p\bar{p} \rightarrow W^\pm b\bar{b} + \text{anything}$, with the two subprocesses $p\bar{p} \rightarrow W^\pm H^0$ ($H^0 \rightarrow b\bar{b}$) and $p\bar{p} \rightarrow tb$ ($t \rightarrow Wb$) [5], which - together with several other SM diagrams - contribute to the $Wb\bar{b}$ final state. Another example is the reaction [6].

$$\gamma \quad e \longrightarrow \nu \quad b \quad \bar{b} \quad W^- \quad (1)$$

Here, three out of 24 SM diagrams, shown in Fig. 1, involve associated Higgs boson production,

$$\gamma \quad e \longrightarrow \nu \quad W^- \quad H^0, \quad (2)$$

and four diagrams represent single top quark production,

$$\gamma \quad e \longrightarrow \nu \quad \bar{t} \quad b, \quad (3)$$

with subsequent decays of the Higgs boson ($H^0 \rightarrow b\bar{b}$) and the top quark ($t \rightarrow Wb$).

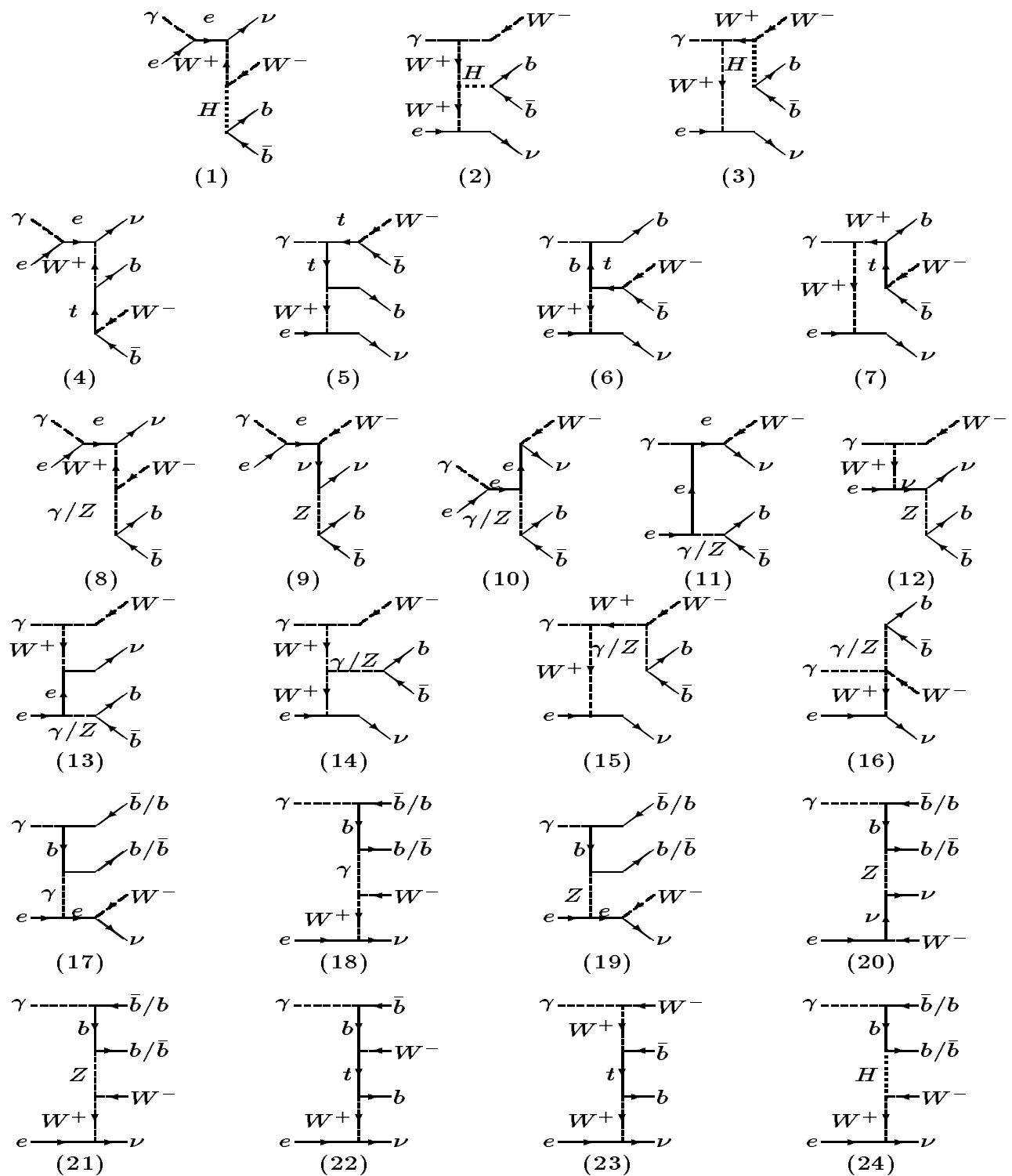


Figure 1: Feynman diagrams for the reaction $\gamma e \rightarrow \nu b\bar{b}W$.

Both reactions have been studied in the past [7, 8] and their abundant rates were emphasized. The associated Higgs production reaction (2) has a large sensitivity for probing anomalous WWH coupling structures [6], whereas the single top reaction (3) is a unique tool for measuring the $|V_{tb}|$ matrix element with very high precision [6, 8, 9].

In this study we present results of complete tree-level calculations of the reaction $\gamma e \rightarrow \nu b \bar{b} W$ including in a model independent way possible anomalous Wtb and HWW couplings. Decays of unstable particles with correct spin structures and contributions from all nonresonant diagrams are taken into account. The subreactions (2) and (3) are involved in the 2-to-4 body calculations and, as will be shown, they can easily be extracted from the inherent background leading to the same final state. In our discussion we will follow basically the papers [6, 10].

The results presented have been obtained by means of the computer package CompHEP 3.2 [11]. As seen from the diagrams in Fig. 1, a number of singularities exists in the s- and t-channels. In the phase space integration by the adaptive Monte Carlo method, a proper treatment of such singular behaviour is necessary in order to obtain stable results. Singularities are smoothed by appropriate transformations of variables, and the procedure of ref. [12] has been adopted in our calculations.

The total cross section for the reaction (1), $\gamma e \rightarrow \nu b \bar{b} W$, and the subprocess contributions are shown in Fig. 2 as a function of $\sqrt{s_{\gamma e}}$ for a Higgs mass of $M_H = 80$ GeV and a top mass of $m_t = 180$ GeV. All cross section rise with increasing energy over the whole energy range considered due to the presence of the t-channel diagrams. If the $\sqrt{s_{\gamma e}}$ is varied in the interval 0.5 - 2.0 TeV, the total cross section and the cross sections for Higgs and top production vary from 110 fb to 630 fb (total), from 45 fb to 290 fb (Higgs, $M_H = 80$ GeV) and from 35 fb to 110 fb (Top, $m_t = 180$ GeV) respectively, and they are large enough to be very interesting for more detailed studies.

However in order to obtain 'realistic' estimations of event rates, the reaction cross sections have to be convoluted with some backscattered photon flux. We have, as an example, adopted in our calculations the widely used photon spectrum (see the paper [13]). The convolution leads to a decrease of the cross section by a factor of 2.5 - 1.5 depending on the collider energy; the rate reduction is larger at smaller energies. After the convolution the total cross section of reaction (1) varies from 40 fb to 420 fb, the Higgs cross section changes from 16 fb to 185 fb for $M_H = 80$ GeV (8 fb to 160 fb for $M_H = 140$) and the top contribution from 14 fb to 90 fb between $\sqrt{s_{\gamma e}} = 0.5 - 2.0$ TeV. It is encouraging that even after such a degradation of the basic cross sections, an electron-photon collider can considerably improve the physical capabilities of Higgs and top studies.

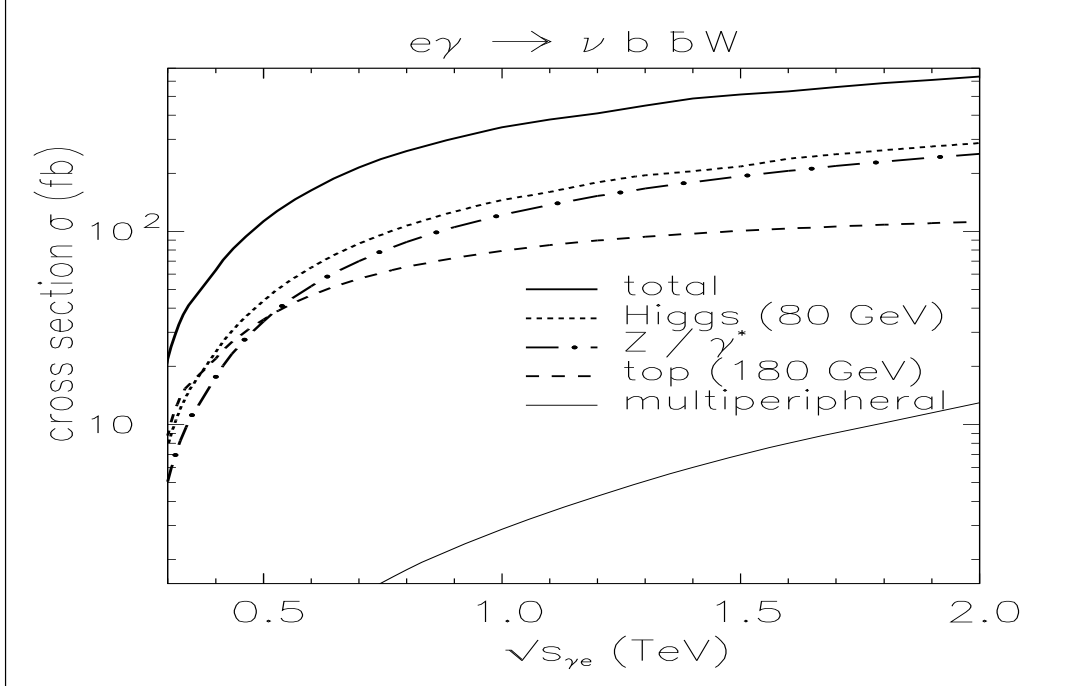


Figure 2: Total cross section for the reaction $\gamma e \rightarrow \nu b \bar{b} W$ as function of the γe cm energy. Also the individual contributions of the Higgs, the top, the Z/γ^* and the multiperipheral diagrams are shown.

2 Wtb coupling

In this section we consider the precision of the measurement for the $|V_{tb}|$ matrix element and a probe of a possible anomalous Wtb coupling in a model independent way.

Measurements of $|V_{tb}|$ or the partial width Γ_{tWb} , which are related in the SM, are known to be nontrivial. The study of the single top quark reaction $e^+e^- \rightarrow e\nu tb$ at high energies [9] offers the possibility to obtain a relatively precise value of $|V_{tb}|$. In this channel, the $|V_{tb}|$ measurement capability relies mainly on the Weizsäcker-Williams photon exchange contributions, $\gamma^* e \rightarrow \nu b t$. Using however the laser backscattered high energy photon beam instead of γ^* the cross sections are typically enhanced by a factor of 3 to 5.

The single top production rate is directly proportional to $|V_{tb}|^2$. However, the top quark is not observed directly; it decays into a W and a b quark, leading to the final state $\nu b \bar{b} W$. There are, as mentioned, several other contributions to the same final state which are not proportional to $|V_{tb}|$. Fortunately, the extraction of the top out of this 4-body final state can be easily achieved with a small loss of the single top rate as seen from Fig. 3, where the invariant masses of the W and the b are shown for four energies. Selection of top events requires only a cut around m_t and no further demands.

Using expected e^+e^- luminosities as proposed in ref. [14], an $e - \gamma$ conversion

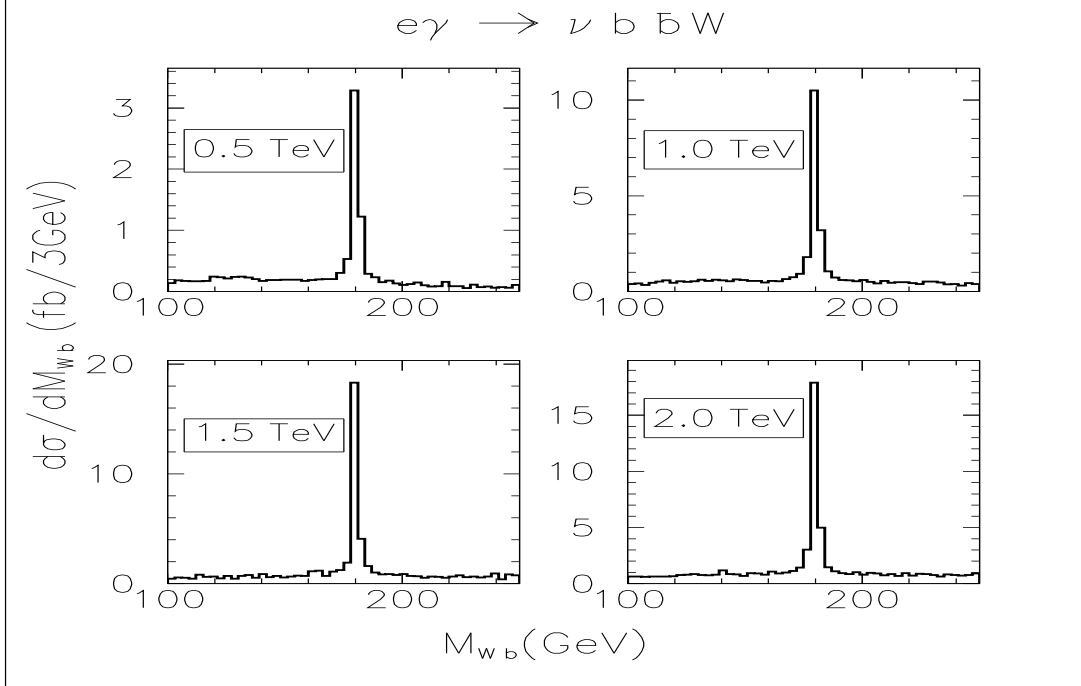


Figure 3: Differential cross sections $d\sigma/dM_{Wb}$ of reaction (1) as function of M_{Wb} .

factor of 0.8 and a 30% $\nu b t$ event detection probability (due to cuts to observe the top decay products and the b -jet and to eliminate backgrounds; major backgrounds are expected from the reactions $\gamma e \rightarrow \nu W Z$ and $\gamma e \rightarrow e W^+ W^-$), the two-standard deviation errors on $|V_{tb}|$ are shown in Tab. 1. As can be seen,

Table 1: Two-standard deviation error of $|V_{tb}|$ expected for the annual luminosities as indicated.

$\sqrt{s_{e^+e^-}}$, TeV	0.5	1.0	1.5	2.0
\mathcal{L} fb $^{-1}$	50	200	300	500
$\delta V_{tb} $	8%	2%	1.5%	1%

the CKM matrix element $|V_{tb}|$ can be probed with high accuracy. Our error obtained at $\sqrt{s_{e^+e^-}}$ of order of 0.5 TeV is similar to the one-standard deviation error expected at the upgraded Tevatron and LHC [15]. However, a higher energy γe collider provides a better determination of $|V_{tb}|$.

In order to probe an anomalous Wtb coupling in a model independent way, we use the effective Lagrangian approach [16, 17] with notations in the unitary gauge as given in ref. [18]. The Lagrangian \mathcal{L} contains only necessary vertices for the process (3):

$$\mathcal{L} = \frac{g}{\sqrt{2}} \left[W_\nu^- \bar{b} (\gamma_\mu F_1^L P_- + F_1^R P_+) t - \frac{1}{2M_W} W_{\mu\nu} \bar{b} \sigma^{\mu\nu} (F_2^L P_- + F_2^R P_+) t \right] + \text{h.c.} \quad (4)$$

with $W_{\mu\nu} = D_\mu W_\nu - D_\nu W_\mu$, $D_\mu = \partial_\mu - ieA_\mu$, $P_\pm = 1/2(1 \pm \gamma_5)$ and $\sigma^{\mu\nu} = i/2(\gamma_\mu\gamma_\nu - \gamma_\nu\gamma_\mu)$. The similarity of the $\sigma^{\mu\nu}$ -connected operators with the QED anomalous magnetic moments prompts the name ‘magnetic type’ for the operators and their associated vertices. Within the Standard Model, $F_1^L = |V_{tb}|$ and $F_1^R = F_2^{L,R} = 0$. Terms containing $\partial_\mu W^\mu$ are omitted in the Lagrangian. They can be recovered by applying the quantum equation of motion through operators of the original Lagrangian [17]. We assume CP conservation with $F_i^{L,R} = F_i^{*L,R}$. The corresponding Feynman rules in the unitary gauge, obtained from the effective Lagrangian, are listed in the Appendix of [10]. These rules for the new vertices have been implemented into the program CompHEP 3.2.

The tree-level diagrams contributing to the subreaction $\gamma e \rightarrow \nu \bar{t} b$ are shown in Fig. 4 where the last non-SM diagram with the four-point $\gamma W tb$ vertex is needed in order to ensure $\mathcal{U}(1)$ gauge invariance. The new vertex $\gamma W tb$ contains the sole contribution from the magnetic type of operators proportional to $F_i^{*L,R}$ and follows from the effective Lagrangian.

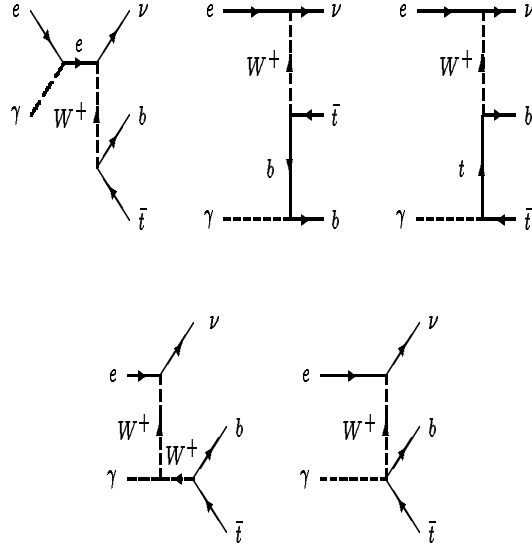


Figure 4: Feynman diagrams for the reaction $\gamma e \rightarrow \nu \bar{t} b$.

Fig.5 shows the variation of the single top cross section as function of the anomalous couplings F_1^R , F_2^L , F_2^R at fixed SM value for $|V_{tb}|$, at four cm energies $\sqrt{s_{e^+e^-}} = 0.5, 1.0, 1.5$ and 2.0 TeV.

Each of the figures 5a-c reflects a possible deviation of the different anomalous couplings around zero with the other F-parameters fixed to the SM-values.

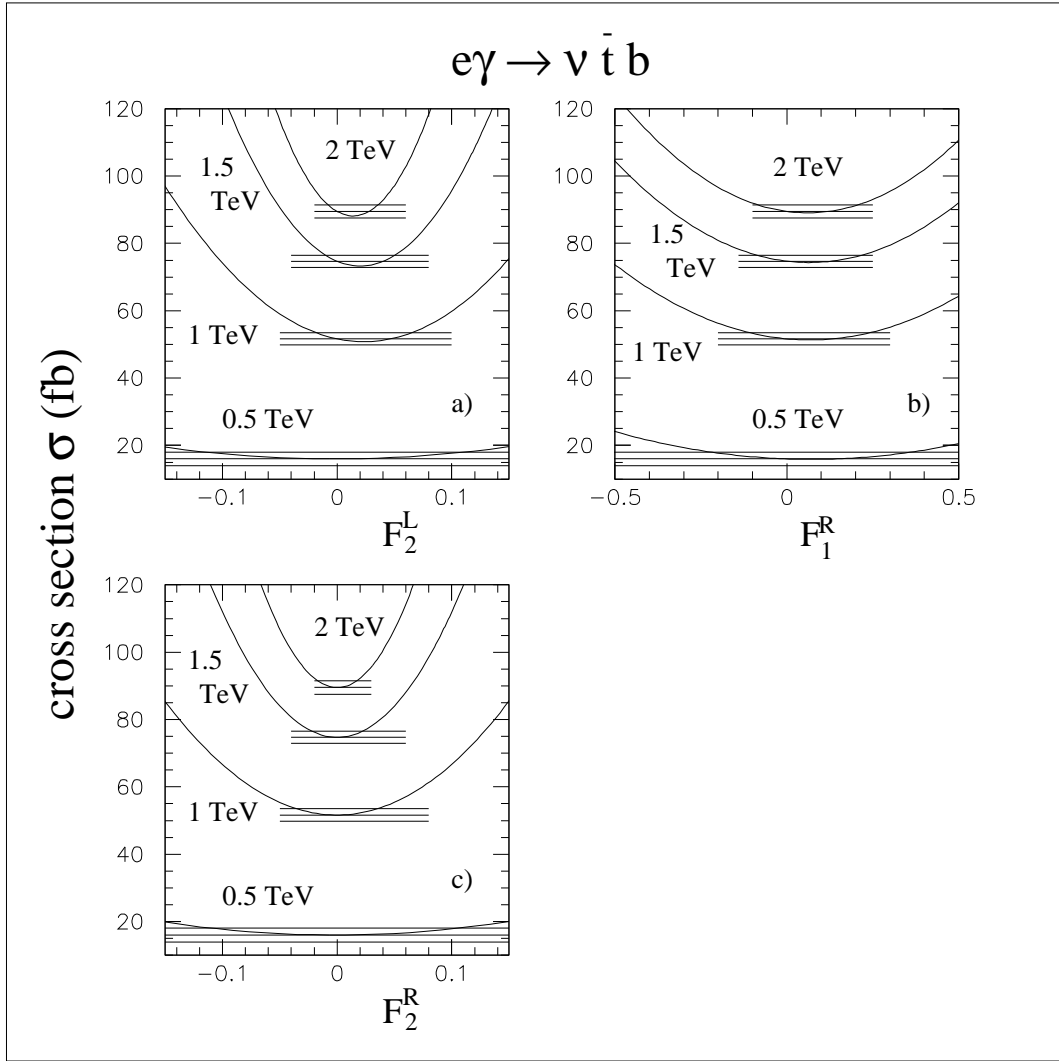


Figure 5: Cross sections of the reaction $\gamma e \rightarrow \nu \bar{t} b$ as functions of the anomalous couplings F_2^L , F_1^R and F_2^R at $\sqrt{s_{e+e^-}} = 0.5, 1.0, 1.5$ and 2.0 TeV. The horizontal lines show the SM values with the two standard deviation errors expected.

A common feature is an increasing sensitivity with growing energies and an enhancement of the cross section when the couplings deviate from the SM value. As expected from the additional power of momentum the $F_2^{L,R}$ couplings represent a much higher sensitivity to variations from the SM than the F_1^R .

With the same luminosities [14] and the event detection efficiency of 30% as above we calculated limits of the variation of F_1^R , F_2^L and F_2^R within two standard deviations of the SM cross section. As can be seen from Table 2, the limits of the anomalous couplings obtained are in the interesting region [4] of

$$\frac{\sqrt{m_b m_t}}{v} \sim 0.1 \quad (5)$$

and do not exceed the unitary violation bounds [19] in the one TeV scale of

$$F_2^{R,L} \sim 0.8 \quad \text{and} \quad F_1^R \sim 0.6. \quad (6)$$

For comparison, recent studies of single top production rates including anomalous couplings [20, 21] indicate the bounds $-0.5 \lesssim F_1^R \lesssim 0.5$ and $-0.1 \lesssim F_2^L \lesssim 0.2$ and $-0.2 \lesssim F_2^R \lesssim 0.2$ [22] which are comparable with our results expected at NLC energies of 0.5 TeV. At energies above 0.5 TeV we obtain significantly higher sensitivities (see Table 2).

$\sqrt{s_{e^+e^-}}$, TeV	0.5	1.0	1.5	2.0
\mathcal{L} , fb^{-1}	50	200	300	500
δF_2^L	-.1/.1	-.020/.065	-.01/.05	-.008/.035
δF_2^R	-.1/.1	-.035/.035	-.022/.022	-.016/.016
δF_1^R	-.20/.35	-.12/.25	-.09/.22	-.08/.20

lous couplings at the Tevatron indicate the bounds $-0.5 \lesssim F_1^R \lesssim 0.5$ [20, 21], $-0.1 \lesssim F_2^L \lesssim 0.2$ and $-0.2 \lesssim F_2^R \lesssim 0.2$ [22] which are comparable with our results expected at NLC energies of 0.5 TeV. At energies above 0.5 TeV we obtain significantly higher sensitivities (see Table 2).

The existence of anomalous couplings also affects production properties of the final state particles of reaction (3). As an example, Fig.6a-c show the differential cross sections $d\sigma/d\cos\Theta_{\gamma b}$, $d\sigma/dp_\perp^t$ and $d\sigma/dp_\perp^b$ expected for $F_2^L = -0.1$, $F_2^R = F_1^R = 0$ and $F_1^L = \text{SM value}$ (open areas), compared with the SM predictions (hatched areas)¹. In particular, the SM angular distribution $d\sigma/d\cos\Theta_{\gamma b}$ in Fig.

¹The angle $\Theta_{\gamma b}$ is defined as the angle of the b -quark with respect to the incident photon direction in the e^+e^- rest frame.

6a has a broad minimum around $\cos\Theta_{\gamma b} \sim 0 - 0.5$. This behavior is due to the existence of the so called radiation zero of the 2-to-2 body process $q\bar{q} \rightarrow W\gamma$ [23] and its time-reversed reaction $\gamma W \rightarrow \bar{t}b$ as the most important subreaction for our consideration. In our case, the incident γ spectrum and the off-shell character of the W -boson in addition to the contribution of the first diagram of Fig. 1 washed out this zero to a broad minimum. Nevertheless, for anomalous coupling contributions the minimum becomes significantly higher.

In the Lagrangian (4), the (V+A) operator which is proportional to the F_1^R coupling has only an overall numerical factor and leads to a simple shift of the p_\perp distributions. On the other hand, as was mentioned the new anomalous magnetic type vertices contain an additional power of momentum (see [10]) and therefore the transverse momentum distributions of the t - and b -quark deviate from the SM expectations. As a consequence, such different behaviour allows to

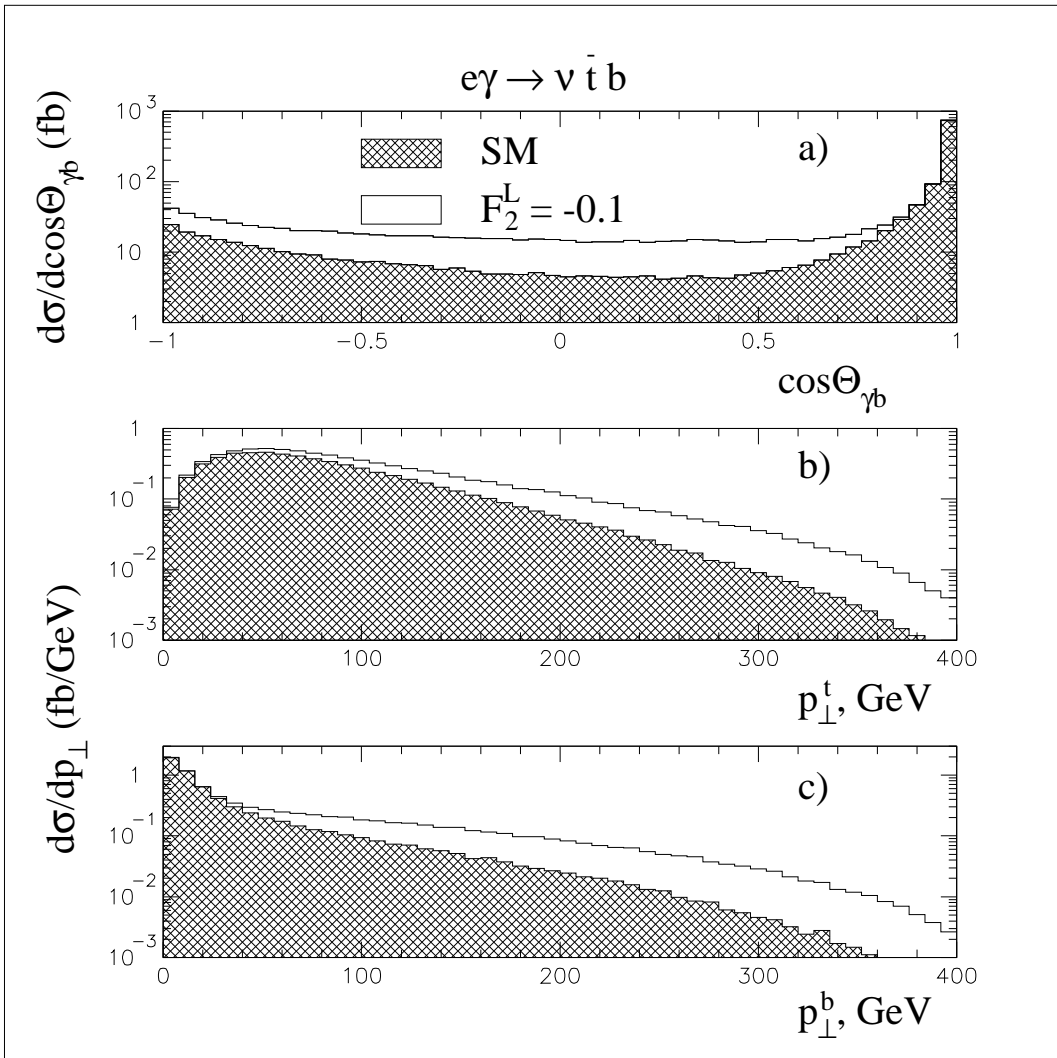


Figure 6: The $\cos\Theta_{\gamma b}$, p_\perp^t and p_\perp^b distributions at 1.0 TeV. Compared are the SM predictions (hatched areas) with expectations from an anomalous coupling $F_2^L = -0.1$.

separate contributions of the (V+A) operator from the magnetic type ones. Fig. 6b and c show an excess at high p_\perp for both, the p_\perp^b and the p_\perp^t distributions. Clearly, cuts in the transverse momenta and angular distributions should lead to significantly more stringent constraints in $F_i^{R,L}$. For illustration purpose, we require $p_\perp^b > 40$ GeV, $p_\perp^t > 80$ GeV and $\Theta_{\gamma b} > 10^0$ for the cross section calculation at 1 TeV. The bounds are improved to $-0.012 < F_2^L < 0.058$ which should be compared with $-0.020 < F_2^L < 0.065$ (see Tab. 2).

A further possibility for studying anomalous couplings could be the measurement of the top quark partial decay width [19] described by the same effective Lagrangian \mathcal{L} . Here, the partial decay width is extracted from the single top production rate and therefore the measurement is not independent from the procedure given above.

An unpolarized $t\bar{t}$ -pair production measurement at hadron collisions would only deliver the branching ratio of the top quark into W -boson and b -quark comparing the single and double b -tagging rates [24]. Calculations show that the branching ratio is very insensitive to variations of the F-parameters. Even for extreme values of the parameters in the range of ± 1 the branching fraction varies from 99.7% to 99.9%. Since the precision of the determination of the branching ratio is of the order of 10%, a deviation from the SM value of 99.8% due to the influence of anomalous couplings will not be visible.

3 Probing the HWW coupling

Reaction (1), $\gamma e \rightarrow \nu b\bar{b}W$, involves also significant Higgs production with a rate directly proportional to the HWW coupling. In the SM the Higgs-vector boson vertices are uniquely determined. In the following we parametrize possible non-SM WWH coupling by introducing an effective non-renormalizable Lagrangian which preserves the SM gauge group

$$\mathcal{L}_{eff} = \mathcal{L}_{SM} + \sum_{k=1}^{\infty} \frac{1}{(\Lambda^2)^k} \sum_i f_i^{(k)} Q_i^{d_k} \quad , \quad (7)$$

where $d_k = 2k+4$ denotes the dimension of operators and Λ is the energy scale of new interactions. We limit ourselves to the complete set of the effective dimension-6 operators as outlined in ref. [16]. Under this restriction phenomenological applications to anomalous Higgs couplings have been discussed in [17]-[25]. One can show that from the four operators involving the WWH coupling there are only two [25] which preserve the custodial $SU(2)$ symmetry [26] relevant for the Higgs subprocess $\gamma e \rightarrow \nu WH$:

$$\frac{1}{\Lambda^2} \left\{ \frac{1}{2} f_\varphi \partial_\mu (\Phi^+ \Phi) \partial^\mu (\Phi^+ \Phi) + f_{WW} \Phi^+ (\hat{W}_{\mu\nu} \hat{W}^{\mu\nu}) \Phi \right\} \quad . \quad (8)$$

Such an effective HWW interaction has been also implemented in the program CompHEP (see the Appendix in [6]) with the following definition of the parameters F_i :

$$F_\varphi/(1TeV^2) = f_\varphi/\Lambda^2 \quad F_{WW}/(1TeV^2) = f_{WW}/\Lambda^2 \quad (9)$$

Probing the HWW coupling involves calculating the dependence of the cross section of the subreaction $\gamma e \rightarrow \nu WH$ on the parameters F_i and comparison with the SM expectation. As in the case of the single top production, the νWH events also can be extracted from the 4-body final state $\nu b\bar{b}W$ of reaction (1) by imposing a cut on the $b\bar{b}$ invariant mass, $M_H - 3 \text{ GeV} < M(b\bar{b}) < M_H + 3 \text{ GeV}$, as seen in Fig. 7. Fig. 8(9) shows the Higgs cross section as function of F_φ (F_{WW})

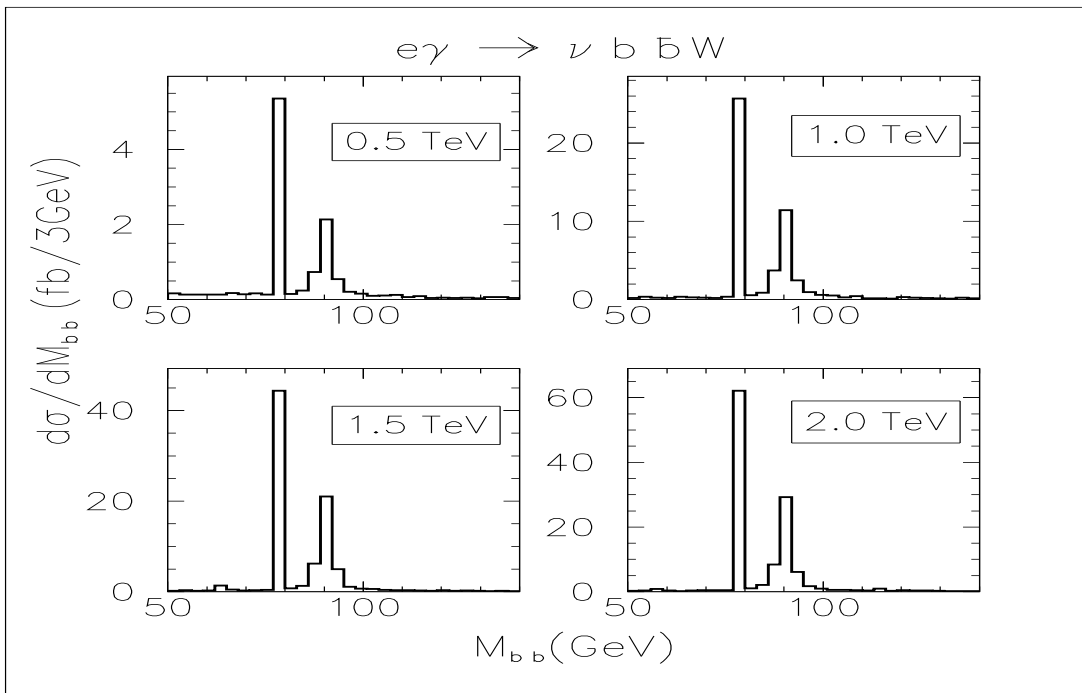


Figure 7: Differential cross sections as a function of the $b\bar{b}$ invariant mass at e^+e^- cm energies of 0.5, 1.0, 1.5 and 2.0 TeV. Clear H^0 and Z peaks are visible on a very small background.

for $F_{WW}(F_\varphi) = 0$, at $\sqrt{s_{e^+e^-}} = 0.5, 1.0, 1.5$ and 2.0 TeV for $M_H = 80 \text{ GeV}$. In order to estimate the ranges of F_i which can be probed within our assumptions, we determined those variations of the F_i which leave the cross section unchanged within 2 s.d. from the SM value. Only statistical errors of the cross sections were considered taking into account once more the integrated luminosities of Tab. 1, an $e - \gamma$ conversion factor of 0.8 and a 30% νHW detection probability. The intervals of F_i obtained are presented in Tab. 3.

Clearly, the larger the cm energy the more sensitive the cross section becomes to a modification of the HWW coupling. The analyses of the two-body reactions $e^+e^- \rightarrow H\gamma$ or HZ [19, 25] revealed higher sensitivities for these operators at

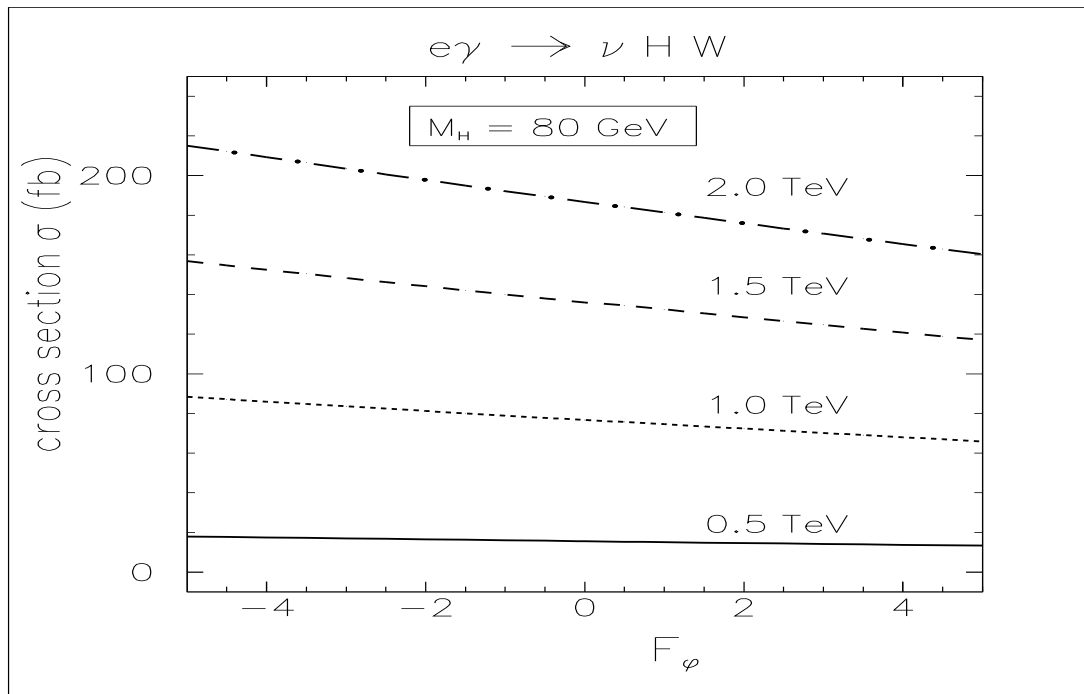


Figure 8: Higgs cross sections as function of the parameter F_φ with $F_{WW} = 0$, at e^+e^- cm energies of 0.5, 1.0, 1.5 and 2.0 TeV for $M_H = 80$ GeV.

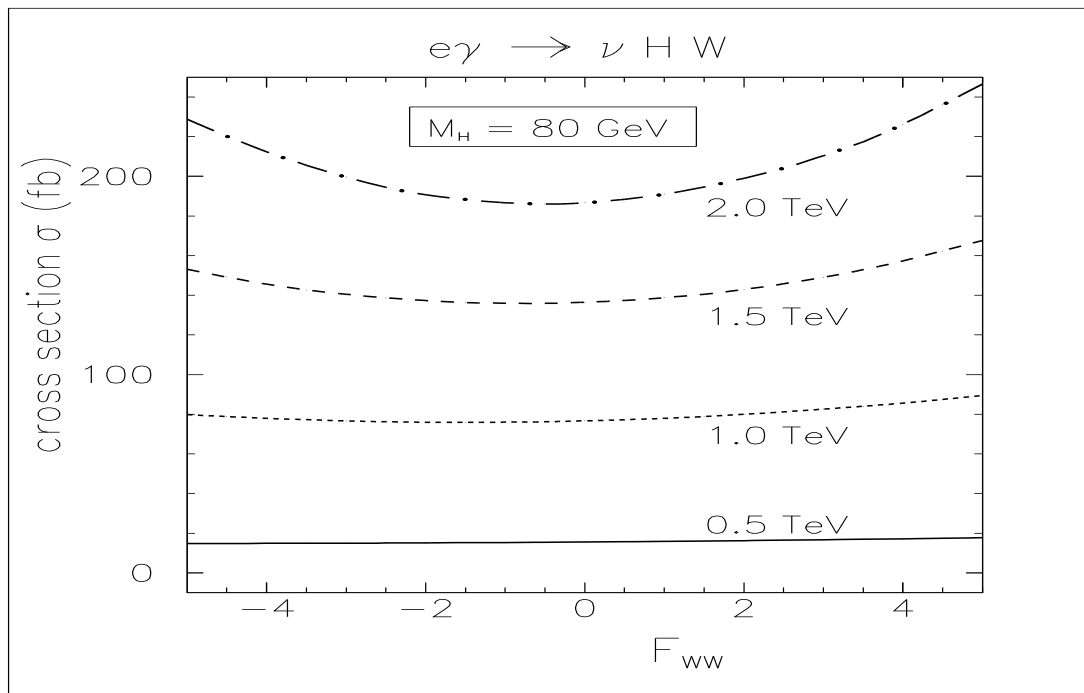


Figure 9: Higgs cross sections as functions of the parameter F_{WW} with $F_\varphi = 0$, at e^+e^- cm energies of 0.5, 1.0, 1.5 and 2.0 TeV for $M_H = 80$ GeV.

Table 3: Range of $|F_\varphi|$ and $|F_{WW}|$ obtained from the two-standard deviation criteria as described in the text.

$\sqrt{s_{e^+e^-}}$, TeV	0.5	1.0	1.5	2.0
$ F_\varphi $	5.0	1.0	0.6	0.4
$ F_{WW} $	9.0	2.5	2.0	1.0
$ F_\varphi $	5.0	1.0	0.6	0.4
$ F_{WW} $	9.0	2.5	2.0	1.0

energies below 1 TeV. At the energies 1-2 TeV the reaction $\gamma e \rightarrow \nu WH$ becomes comparable or slightly more sensitive.

4 Summary

Results [6, 10] of the complete tree-level calculation of the reaction $\gamma e \rightarrow \nu b \bar{b} W$ at cm energies 0.5 to 2.0 TeV are presented and discussed. The reaction is very interesting on its own because it involves at the same time single top production, $\gamma e \rightarrow \nu \bar{b} t$, and associated Higgs production, $\gamma e \rightarrow \nu HW$, with subsequent decays of $t \rightarrow Wb$ and $H \rightarrow b \bar{b}$, respectively. Therefore, both three-body sub-reactions already studied in previous publications are analyzed in an extended manner taking into account interferences between different subchannels, the irreducible background, and contributions from the anomalous Wtb and HWW couplings. It is demonstrated that both subreactions can be easily extracted from the 4-body final state.

The event rate for the reaction $\gamma e \rightarrow \nu tb$, which is large even after folding with an energy spectrum of the backscattered photon beam and making reasonable assumptions on collider luminosities and detection probabilities, provides the best sensitive measurement, compared to other collision processes, for the CKM matrix element $|V_{tb}|$ as well as for probing the anomalous Wtb couplings in a model independent way.

The reaction $\gamma e \rightarrow \nu HW$ allows to probe the HWW coupling and to measure parameters of dimension-6 operators in the effective Lagrangian. It has been found that at 0.5 TeV the accuracy obtained on these parameters is not

sufficient to make this measurement sensitive to new physics while at energies $\sqrt{s_{e^+e^-}} = 1\text{-}2$ TeV the HWW coupling can be probed with high sensitivity and deviations from the Standard Model could show up.

Acknowledgments

The work has been supported in part by the RFBR grant 96-02-19773a, and by the grant 95-0-6.4-38 of the Center for Natural Sciences of State Committee for Higher Education in Russia. E.B. is grateful to the Deutsche Forschungsgemeinschaft (DFG) for the financial support.

References

- [1] P. Grannis, plenary talk at the International Conference on High Energy Physics, Warsaw, 1996.
- [2] A. Blondel, plenary talk at the International Conference on High Energy Physics, Warsaw, 1996, CERN Report No. LEPEWWG/96-02.
- [3] I. Bigi, Y. Dokshitzer, V. Khose, J. Kühn and P. Zerwas, Phys. Lett. **B181** (1986) 157.
- [4] R.D. Peccei and X. Zhang, Nucl. Phys. **337** (1990) 269;
R.D. Peccei, S. Peris and X. Zhang, Nucl. Phys. **349** (1991) 305.
- [5] A. Belyaev, E. Boos and L. Dudko, Mod. Phys. Lett. **A10** (1995) 25.
- [6] E. Boos, A. Pukhov, M. Sachwitz and H.J. Schreiber, Z. Phys. **C75** (1997) 237.
- [7] E. Boos, M. Dubinin, V. Ilyin, G. Jikia, A. Pukhov and S. Sultanov, Phys. Lett. **B273** (1991) 173;
K. Hagiwara, I. Watanabe and P.M. Zerwas, Phys. Lett. **B278** (1992) 187;
K. Cheung, Phys. Rev. **D48** (1993) 1035.
- [8] G. Jikia, Nucl. Phys. **B374** (1992) 83;
E. Yehudai, S. Godfrey and K.A. Peterson, Proc. of the Workshop on Physics and Experiments with Linear e^+e^- Colliders, Waikoloa, Hawaii, April 26-30, 1993, p.569.
- [9] E. Boos, Y. Kurihara, Y. Shimizu, M. Sachwitz, H.J. Schreiber and S. Shichanin, Z. Phys. **C70** (1996) 255.

- [10] E. Boos, A. Pukhov, M. Sachwitz and H.J. Schreiber, Phys. Lett. **B404** (1997) 119.
- [11] E. Boos, M. Dubinin, V. Ilyin, A. Pukhov and V. Savrin, hep-ph/9503280, SNUTP-94-116;
P. Baikov et al., in Proc. of the Xth Int. Workshop on High Energy Physics and Quantum Field Theory, QFTHEP-95, ed. by B. Levchenko and V. Savrin, (Moscow, 1995), p.101.
- [12] V.A. Ilyin, D.N. Kovalenko, and A.E. Pukhov, Int. Mod. Phys. **C7** (1996) 761;
D.N. Kovalenko and A.E. Pukhov, Nucl. Instr. and Meth. **A389** (1997) 299.
- [13] I.F. Ginzburg, G.L. Kotkin, V.G. Serbo and V.I. Telnov, Pisma ZhETF 38 (1981) 514;
V.I. Telnov, Nucl. Instr. and Meth. **A294** (1990) 72.
- [14] B.H. Wiik, talk given at the TESLA meeting, Frascati, Nov. 1994.
- [15] A.P. Heinson, A.S. Belyaev and E.E. Boos, Proc. of the Workshop on Physics of the Top Quark, Iowa State University, Ames, Iowa (1995);
D.O. Carlson and C.-P., Proc. of the Workshop on Physics of the Top Quark, Iowa State University, Ames, Iowa (1995);
T. Stelzer and S. Willenbrock, Phys. Lett. **B357** (1995) 125;
S. Willenbrock, talk given at the 28th International Conference on High Energy Physics, 25-31 July 1996, Warsaw, Poland.
- [16] W. Buchmüller and D.Wyler, Nucl. Phys. **B268** (1986) 621.
- [17] K. Hagiwara, S. Ishihara, R. Szalaski and D. Zeppenfeld, Phys. Rev. **D48** (1993) 2182;
K. Hagiwara, R. Szalaski and D. Zeppenfeld, Phys. Lett. **B318** (1993) 155;
B. Grzadkowski and J. Wudka, Phys. Lett. **B364** (1995) 49;
G.J. Gounaris, F.M. Renard and N.D. Vlachos, Nucl. Phys. **B459** (1996) 51;
G.J. Gounaris, J.Layssac, J.E. Paschalis, F.M. Renard and N.D. Vlachos, preprint PM/96-08 and THEP-TP 96/02.
- [18] G. L. Kane, G.A. Ladinsky and C.-P. Yuan, Phys. Rev. **D45** (1992) 124.
- [19] G.J. Gounaris, M. Kuroda and F.M. Renard, Phys. Rev. **D54** (1996) 6861;
G.J. Gounaris, D.T. Papadamou and F.M. Renard, PM-96-28, Sept 1996 and hep-ph/9609437.

- [20] F. Larios, E. Malkawi, C.P. Yuan, Talk given at CCAST Workshop on Physics at TeV Energy Scale, Beijing, China, 15-26 Jul 1996.
- [21] A.P. Heinson, A.S. Belyaev and E.E. Boos, Phys. Rev. **D56** (1997) 3114.
- [22] E. Boos, M. Dubinin, L.Dudko in preparation.
- [23] Dong-pei Zhu, Phys. Rev. **D22** (1980) 2266;
M.A. Samuel, Phys. Rev. **D27** (1983) 2724.
- [24] D. Amidai and C. Brock, Report of the TeV 2000 Study Group on Future Electroweak Physics at the Tevatron, 1995.
- [25] W. Kilian, M. Krämer and P.M. Zerwas, Phys. Lett. **B381** (1996) 243.
- [26] P. Sikivie, L. Susskind, M. Voloshin and V. Zakharov, Nucl. Phys. **B173** (1980) 189.